

Model-agnostic Selective Labeling with Provable Statistical Guarantees

Huipeng Huang ^{*1} Wenbo Liao ^{*12} Huajun Xi ¹ Hao Zeng ¹ Mengchen Zhao ³ Hongxin Wei ¹

Abstract

Obtaining high-quality labels for large datasets is expensive, requiring massive annotations from human experts. While AI models offer a cost-effective alternative by predicting labels, their predictions inevitably contain errors. Existing methods mitigate this issue through selective labeling, where AI labels a subset and experts label the rest. However, these methods lack rigorous theoretical guarantees on the quality of AI-assigned labels, potentially leading to substantial labeling errors. To address this, we propose **Conformal Labeling**, a novel and model-agnostic method to identify a subset of unlabeled data with strict false discovery rate (FDR) control. In particular, we leverage a small labeled calibration set to construct conformal p -values for test data and estimate the accuracy of AI models. Then, we determine a data-dependent threshold for p -value selection, which automatically adapts to the estimated accuracy—higher accuracy permits a larger threshold. We provide theoretical guarantees that Conformal Labeling controls the FDR below the nominal level, ensuring that a predefined fraction of AI-assigned labels is correct in expectation. Extensive experiments across a wide range of models and datasets demonstrate that our method can achieve the target labeling quality with high power in classification and open-ended generation tasks.

1. Introduction

Large-scale, high-quality labeled data is crucial for the machine learning pipelines (Deng et al., 2009). While human experts can provide reliable annotations for moderately sized datasets, the rapid growth of modern datasets has rendered this approach prohibitively expensive. AI models

offer a cost-effective alternative by predicting labels. However, AI models are prone to labeling error (Northcutt et al., 2021; Tan et al., 2024), with empirical evidence showing that state-of-the-art LLMs exhibit high error in text annotation tasks (Baumann et al., 2025). The prediction errors compromise label quality, hindering the deployment of AI labeling in real-world applications. To balance the trade-off between labeling cost and error, selective labeling has been a promising solution (Li et al., 2023; Wang et al., 2023) by combining AI predictions with expert annotations.

Prior work on selective labeling primarily designed heuristic methods (Wang et al., 2021; Bernhardt et al., 2022; Wang et al., 2024a). These methods typically rely on model confidence, assigning high-confidence instances to AI models while deferring the remaining instances to human experts. However, these methods provide no theoretical guarantee on label quality. When the AI model is inaccurate or the confidence measure is unreliable, a substantial number of incorrect AI-assigned labels will be introduced, leading to a low-quality labeled dataset. Explicit accuracy guarantees directly address this issue by quantifying and controlling the quality of AI-assigned labels, ensuring that the resulting labeled dataset has a bounded error level pre-defined by users. This motivates us to design a model-agnostic method with provable accuracy guarantees on the AI-assigned labels.

In this work, we propose **Conformal Labeling**, a novel method to identify a subset of unlabeled data with provable FDR control. In particular, we leverage a small labeled calibration set to construct conformal p -values for test data and estimate the accuracy of the AI model. Motivated by our analysis of the conservatism of the Benjamini–Hochberg (BH) procedure (Benjamini & Hochberg, 1995), we apply the BH procedure at an adjusted significance level derived from the estimated model accuracy, which enables effective FDR control while achieving high selection power. We provide theoretical guarantees that Conformal Labeling controls the FDR with distribution-free, finite-sample guarantees. While the error rate of AI labeling in current methods depends heavily on model performance, Conformal Labeling can control the desired labeling error in expectation regardless of the underlying model’s performance.

We empirically validate our method through extensive experiments conducted on three labeling tasks, including im-

^{*}Equal contribution ¹Department of Statistics and Data Science, Southern University of Science and Technology ²Department of Mathematics, The Chinese University of HongKong ³School of Software Engineering, South China University of Technology. Correspondence to: Hongxin Wei <weihx@sustech.edu.cn>.

age labeling (ImageNet (Deng et al., 2009), ImageNet-V2 (Recht et al., 2019)), LLM QA (MedMCQA (Pal et al., 2022), MMLU (Hendrycks et al., 2021), MMLU-Pro (Wang et al., 2024a)), and LLM open-ended generation (MMLU-Redux (Gema et al., 2025), MATH-500 (Lightman et al., 2023) MATH-L5 (Hendrycks et al., 2021), Zebra-Logic (Lin et al., 2025), and HumanEval⁺ (Liu et al., 2023)) tasks. The results demonstrate that Conformal Labeling achieves high power with controlled FDR, indicating that AI models can label a large proportion of data with high quality. For example, Conformal Labeling can label 63.73% of Zebra-Logic with Qwen3-4B-Thinking-2507 (Yang et al., 2025), while controlling the FDR at 9.85%. In comparison, using AI-assigned labels for the entire dataset results in labeling errors of over 10%. Moreover, through comprehensive analyses, we validate that Conformal Labeling is robust to the size of calibration datasets, and the logits-based uncertainty score performs better than the verbalized uncertainty score.

We summarize our contributions as follows:

- We propose Conformal Labeling, a novel method for identifying a subset where AI predictions could be provably trusted. Regardless of AI models’ performance, Conformal Labeling guarantees the quality of AI-assigned labels by strictly controlling the FDR.
- We theoretically prove that Conformal Labeling provides a strict quality guarantee for AI-assigned labels: it achieves FDR control, ensuring the expected portion of incorrect labels is below a user-specified level.
- We empirically show that Conformal Labeling can label a large portion of data with AI models while tightly controlling the FDR, through extensive experiments conducted on image labeling, LLM QA, and LLM open-ended generation tasks with various models.

2. Preliminaries

Problem setup. We study the problem of identifying a subset where AI predictions can be provably trusted. Here, we give a formulation of multi-class classification as an example, while our framework also applies to open-ended generation. Let \mathcal{X} denote the feature space and $\mathcal{Y} = \{1, \dots, K\}$ denote the label space. The test dataset $\mathcal{D}_{\text{test}} = \{X_j\}_{j=1}^m$ consists of m data instances, sampled i.i.d. from a data distribution $\mathcal{P}_{\mathcal{X}}$. We denote the unseen ground-truth labels of instance X_j as Y_j . Besides, we consider a pre-trained AI model $f : \mathcal{X} \rightarrow \mathbb{R}^{|\mathcal{Y}|}$ used to predict labels for the test dataset. For a given test instance X , the AI model predicts the label with the largest estimated probability $\hat{Y} = \arg \max_{y \in \mathcal{Y}} f_y(X)$, where $f_y(X)$ denotes the estimated class probability for class $y \in \mathcal{Y}$.

Since AI models unavoidably make errors when used for

labeling, we aim to select a large subset from the test dataset $\mathcal{D}_{\text{label}}$ to control the portion of incorrect labels. Formally, our goal is to identify the largest subset of indices $\mathcal{R} \subseteq \{1, \dots, m\}$ that controls the FDR, defined as below:

$$\text{FDR} = \mathbb{E} \left[\frac{|\mathcal{R} \cap \mathcal{H}_0|}{\max(|\mathcal{R}|, 1)} \right], \quad (1)$$

where $\mathcal{H}_0 = \{j \in \{1, \dots, m\} : Y_j \neq \hat{Y}_j\}$ is the set of indices with incorrect predictions, and the expectation is taken over the randomness of the data. For notation shorthand, we denote $[m] = \{1, \dots, m\}$ in the following. The FDR metric measures the expected proportion of mislabeled samples within the AI-labeled subset, illustrating the quality of AI-assigned labels by explicitly bounding the expected fraction of incorrect labels.¹

In addition to FDR control, we also expect AI models to label as many test instances as possible correctly, which corresponds to maximizing power:

$$\text{Power} = \mathbb{E} \left[\frac{|\mathcal{R} \cap \mathcal{H}_1|}{\max(|\mathcal{H}_1|, 1)} \right], \quad (2)$$

where $\mathcal{H}_1 = \{j \in [m] : Y_j = \hat{Y}_j\}$ is the set of indices where the AI prediction is correct. It should be emphasized that our method prioritizes FDR control over power, in that we strictly enforce $\text{FDR} \leq \alpha$ to guarantee label quality while optimizing power under the constraints.

In this work, we assume access to a small labeled calibration dataset $\mathcal{D}_{\text{cal}} = \{(X_i, Y_i)\}_{i=1}^n$. For convenience, we denote the test dataset as $\mathcal{D}_{\text{test}} = \{(X_j, Y_j)\}_{j=n+1}^{n+m}$, where Y_j is not observed. Since the labeling cost of a small dataset by human annotators is typically affordable, this assumption is practical in the real world and is also adopted in prior work (Candès et al., 2025). Besides, we assume that examples of the test and calibration datasets are both drawn i.i.d. from the joint distribution $\mathcal{P}_{\mathcal{XY}}$. This assumption is realistic in our setting because we sample the calibration set from a large unlabeled dataset and leave the remaining data for testing. The process ensures that calibration data and test data are naturally i.i.d. In Appendix I.1, we test our proposed method against distribution shift to show that our proposed method is empirically robust to distribution shift.

Selective labeling methods and their limitations. Ensuring high-quality labels while reducing annotation costs has motivated extensive research on selective labeling. Prior work on selective labeling primarily focused on heuristic methods. For example, several works explore human-LLM collaboration for annotation, including uncertainty-guided work allocation (Li et al., 2023), verifier-based qual-

¹The realized FDR might exceed the target level for a single run.

ity assessment that routes low-confidence samples to humans (Wang et al., 2024b), and unsupervised collaboration between LLMs and small models (Xiao et al., 2023).

These methods balance labeling cost and quality by empirically selecting confidence thresholds to route samples between AI models and human annotators, yet provide no theoretical guarantees on the reliability of the AI-assigned labels. These methods implicitly assume well-calibrated confidence scores and sufficiently strong underlying model performance. However, commonly used confidence measures—including softmax probabilities from deep neural networks, logit-based confidence scores from LLMs, and LLM-generated verbalized confidence—are known to be poorly calibrated and overconfident (Guo et al., 2017; Chhikara, 2025), making them unreliable. Moreover, when the underlying model exhibits limited accuracy, even predictions assigned high confidence may be incorrect. Consequently, when the models are inaccurate or the confidence measure is unreliable, these methods will result in substantial labeling errors. These limitations motivate us to explore model-agnostic methods that can provably guarantee the quality of AI-assigned labels in selective labeling.

3. Method

3.1. Conformal Labeling

Our previous section shows that existing methods cannot guarantee the quality of AI-assigned labels. To address this, we propose **Conformal Labeling**, a model-agnostic method to identify a subset where AI predictions can be provably trusted by controlling the FDR. Our method is composed of three primary steps: quantifying uncertainty, constructing conformal *p*-values, and thresholding.

Uncertainty quantification. Our method builds on a key insight: we should select instances where the model exhibits high confidence in its predictions. To quantify the model confidence, we define an uncertainty (non-conformity) score $\mathcal{S} : \mathcal{X} \rightarrow \mathbb{R}$, where a higher value indicates greater model uncertainty. For example, we employ $\mathcal{S}(X) = 1 - \max_{y \in \mathcal{Y}} f_y(X)$ as our uncertainty score function (Hendrycks & Gimpel, 2016). This score is a valid measure of uncertainty, since prior works establish that misclassified samples generally receive lower probability scores (i.e., $\max_{y \in \mathcal{Y}} f_y(X)$) than correctly classified ones (Hendrycks & Gimpel, 2016; Tu et al., 2024).

Statistical guarantee via conformal *p*-value. To provide a statistical guarantee, we reformulate our problem as the following multiple hypothesis testing problem:

$$H_j^0 : \hat{Y}_{n+j} \text{ is incorrect} \quad \text{v.s.} \quad H_j^1 : \hat{Y}_{n+j} \text{ is correct.}$$

The correctness of AI-assigned labels depends on the task definition. For image labeling tasks, correctness is defined as $\hat{Y}_{n+j} = Y_{n+j}$. For open-ended verifiable tasks, correctness corresponds to the generated output being a correct solution. For alignment tasks, correctness means that the generated output aligns with human preferences.

In the formulation, it is worth noting that rejecting the null hypothesis H_j^0 indicates that (X_{n+j}, \hat{Y}_{n+j}) should be included in the selection subset, as \hat{Y}_{n+j} is deemed to be correct. To construct the selection subset, we employ *conformal p-value*, which builds upon the conformal inference framework (Vovk et al., 1999; 2005). The underlying intuition is that: *a test instance X is likely to be misclassified if its uncertainty score $\mathcal{S}(X)$ is generally larger than the scores of instances that are known to be misclassified*. Leveraging this idea, conformal *p*-value is computed through a rank-based comparison of $\mathcal{S}(X)$ against uncertainty scores of misclassified instances.

Formally, for the calibration dataset \mathcal{D}_{cal} , we identify the subset $\mathcal{D}_{cal}^0 \subseteq \mathcal{D}_{cal}$ where instances are misclassified by the AI model. For simplicity, we denote $\mathcal{D}_{cal}^0 = \{(X_i, Y_i)\}_{i=1}^{n_0}$, and thus \hat{Y}_i is incorrect for $i = 1, \dots, n_0$. We compute the uncertainty scores for the entire dataset $\{(X_i, Y_i)\}_{i=1}^{n+m}$: $\mathcal{S}_i = 1 - \max_{y \in \mathcal{Y}} f_y(X_i)$. Then, the conformal *p*-value for the instance X_{n+j} is computed by

$$\hat{p}_j = \frac{\sum_{i=1}^{n_0} \mathbf{1}\{\mathcal{S}_i < \mathcal{S}_{n+j}\} + U_j (1 + \sum_{i=1}^{n_0} \mathbf{1}\{\mathcal{S}_i = \mathcal{S}_{n+j}\})}{n_0 + 1}, \quad (3)$$

where $U_j \sim \text{Uniform}[0, 1]$ are i.i.d. uniform random variable to break ties. Here, \hat{p}_j quantifies how extreme the uncertainty of X_{n+j} is compared to the scores of mislabeled instances, with a small \hat{p}_j providing strong statistical evidence for correct prediction.

The conformal *p*-value defined in (3) has a distribution-free finite-sample guarantee, which is formalized in the following proposition. The conservatism property indicates that the conformal *p*-values for misclassified instances are biased to be high as they stochastically dominate the uniform distribution on $[0, 1]$. This allows us to set a threshold to flag potential correct instances, while controlling the FDR.

Proposition 3.1. (from Vovk et al. (2005)). *Given that the calibration sample $\{(X_i, Y_i)\}_{i=1}^n$ together with the j -th test sample (X_{n+j}, Y_{n+j}) are i.i.d. for $j \in \{1, \dots, m\}$, conformal *p*-value \hat{p}_j defined in (3) is conservative:*

$$\mathbb{P}\{\hat{p}_j \leq \alpha \mid H_j^0 \text{ is true}\} \leq \alpha, \quad \text{for all } \alpha \in (0, 1). \quad (4)$$

Thresholding. After obtaining conformal *p*-values for test instances, we can naively apply the Benjamini–Hochberg (BH) procedure (Benjamini & Hochberg, 1995) as in conformal selection (Jin & Candès, 2023) to select a subset \mathcal{R} for

Algorithm 1 Conformal Labeling

Input: Calibration set $\mathcal{D}_{\text{cal}} = \{(X_i, Y_i)\}_{i=1}^n$, unlabeled test instances $\{X_{n+j}\}_{j=1}^m$, pre-trained model f , target FDR level $\alpha \in (0, 1)$

Output: A selected subset \mathcal{R} with FDR control

- 1: // Identify mislabeled calibration data
- 2: Identify $\mathcal{D}_{\text{cal}}^0 \subseteq \mathcal{D}_{\text{cal}}$ with size n_0
- 3: // Step 1: Compute uncertainty scores
- 4: **for** $i = 1$ to $n + m$ **do**
- 5: Compute uncertainty score \mathcal{S}_i
- 6: **end for**
- 7: // Step 2: Construct conformal p-values
- 8: **for** $j = 1$ to m **do**
- 9: Construct conformal p-value \hat{p}_j according to Eq. (3)
- 10: **end for**
- 11: // Step 3: Thresholding
- 12: Compute $j^* = \max \left\{ j : \hat{p}_{(j)} \leq \frac{\alpha j(n+1)}{m(n_0+1)} \right\}$, where $\hat{p}_{(j)}$ is the j -th smallest p-value.
- 13: **Return** $\mathcal{R} = \{j : \hat{p}_j \leq \hat{p}_{(j^*)}\}$

AI labeling while controlling the FDR at level α . Concretely, let $p_{(1)} \leq \dots \leq p_{(m)}$ denote the ordered statistics of the p -values; the rejection set of the BH procedure applied to the conformal p -values is $\mathcal{R} = \{j : \hat{p}_j \leq \hat{p}_{(j^*)}\}$, where

$$j^* = \max \left\{ j : \hat{p}_{(j)} \leq \frac{\alpha j}{m} \right\}, \quad (5)$$

with the convention that $\max \emptyset = 0$. Under the i.i.d. data assumption, applying the BH procedure to these p -values controls FDR below $\pi_0 \alpha$ (Benjamini & Yekutieli, 2001; Bates et al., 2023), where π_0 is the proportion of incorrect predictions in the test dataset. While this result ensures valid FDR control, it also implies that the effective FDR level of the BH procedure is conservative by a factor of π_0 . When the deployed AI model is often accurate, π_0 is small. As a result, the BH procedure controls the FDR at a level far below the nominal target α , leading to overly conservative thresholding and, consequently, a reduced number of instances selected for labeling.

To mitigate this conservatism issue, we estimate π_0 from the calibration dataset, building upon the intuition that when the calibration data and test data are i.i.d., the model should achieve comparable accuracy on both datasets. In particular, we estimate π_0 with $\frac{1+n_0}{1+n}$, and subsequently apply the BH procedure at level $\frac{1+n}{1+n_0} \alpha$. We summarize the complete procedure of Conformal Labeling in Algorithm 1, which combines all three steps described above.

In Theorem 3.2, we establish that Conformal Labeling controls the FDR below the target level α even when it applies the BH procedure at level $\frac{1+n}{1+n_0} \alpha$. This result provides a formal guarantee that the AI-assigned labels within the se-

lected subset are trustworthy, in the sense that the expected proportion of incorrect labels is bounded by α . Because the BH procedure is applied at an elevated level, Conformal Labeling selects more samples than naively applying the BH procedure at level α . Moreover, Conformal Labeling's upper bound for FDR is tight: it converges to α as the calibration set size increases and equals α in the asymptotic limit. The proof is provided in Appendix A.2.

Theorem 3.2. Suppose the calibration samples $(X_i, Y_i)_{i=1}^n$ and test samples $(X_{n+j}, Y_{n+j})_{j=1}^m$ are i.i.d. Let $\alpha \in (0, 1)$ be the target FDR level, and suppose the selection set \mathcal{R} is determined by Algorithm 1 applied at the target FDR level α . Define $p = \mathbb{E}[H_j^0]$, the probability that a test sample (X_{n+j}, Y_{n+j}) is incorrectly predicted. Taking expectation over the randomness of the calibration and test data, the FDR of the selection set \mathcal{R} satisfies:

$$\text{FDR} \leq [1 - (1 - p)^{n+1}] \alpha \leq \alpha.$$

3.2. Choice of uncertainty score

In the above analysis, we establish that Conformal Labeling controls the FDR below the desired level. However, this guarantee alone is insufficient: a trivial procedure that simply labels nothing would achieve a perfect FDR of 0, yet offer no practical value. This highlights the need to also evaluate the method's statistical power, which measures the method's ability to identify as many correctly labeled instances as possible (see Eq. (2)).

As shown in prior work (Jin & Candès, 2023; Gui et al., 2024; Bai et al., 2025), the statistical power of this method depends on the quality of the uncertainty score. In particular, a score that better separates correct from incorrect predictions directly increases statistical power (see Proposition 7 of Jin & Candès (2023)). To deliver practical recommendations, we empirically compare several uncertainty scores by visualizing their resulting p -value distributions and measuring the final statistical power employed with our method in Figure 1. We utilize a pre-trained ResNet-34 model on the ImageNet dataset, with three uncertainty scores: maximum softmax probability (MSP) (Hendrycks & Gimpel, 2016), energy score (Liu et al., 2020), and DOCTOR- α score (D_α) (Granese et al., 2021). We give an overview of these score functions in Appendix B. The results show that both MSP and D_α score provide a clear distinction between correct and incorrect predictions, thus achieving high statistical power. However, the energy score fails to provide this separation, leading to low power. Given the comparable power performance of MSP and D_α score, we will use the more computationally efficient MSP in our main experiments. In Appendix I.2, we provide a detailed comparison of the power and FDR achieved by these score functions.

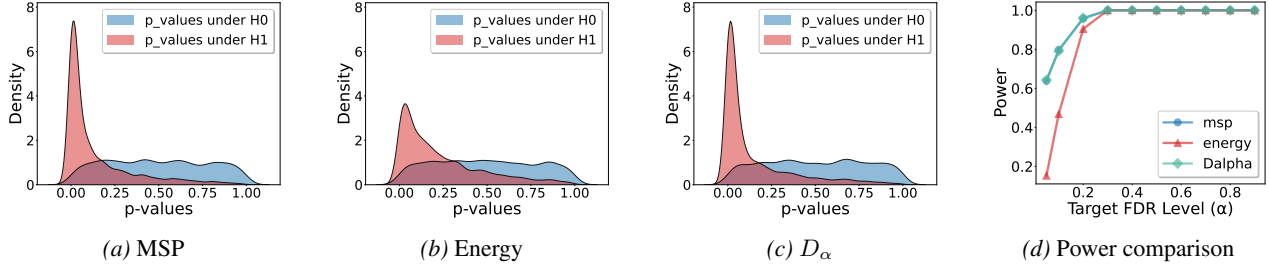


Figure 1. Empirical distributions and power (employed with our method) of conformal p -values under different uncertainty scores. The experiments include maximum softmax probability (MSP), energy, and DOCTOR- α score (D_α). The experiments are conducted on ImageNet with ResNet-34. The results show that both MSP and D_α score create a clear distinction between correct and incorrect predictions, thus achieving high statistical power. However, the energy score fails to provide this separation, leading to low power.

4. Experiments

In this section, we evaluate the effectiveness of Conformal Labeling on image labeling, LLM QA, and LLM open-ended generation tasks with various models. We find that it achieves tight FDR control and high power, indicating that AI models can label a large proportion of data with bounded error. In addition, we conduct additional analyses to provide practical guidance for applying our method.

4.1. Experimental setup

Datasets. We conduct experiments on image labeling, LLM QA, and LLM open-ended generation tasks. For image labeling, we use ImageNet (Deng et al., 2009) and ImageNet-V2 (Recht et al., 2019). For LLM QA task, we use MedMCQA (Pal et al., 2022), MMLU (Hendrycks et al., 2021), and MMLU-Pro (Wang et al., 2024c). For LLM open-ended generation task, we use MMLU-Redux (Gema et al., 2025), MATH-500 (Lightman et al., 2023), MATH-L5 (Hendrycks et al., 2021), Zebra-Logic (Lin et al., 2025), and HumanEval⁺ (Liu et al., 2023) to evaluate Conformal Labeling’s performance in general, math reasoning, text reasoning and coding tasks respectively. We also show how to extend our method to regression tasks in Appendix H.

Models. We conduct extensive experiments on various open-sourced AI models. For image labeling, we use ResNet-34 (He et al., 2016), DenseNet-161 (Huang et al., 2018), and a Vision-Language Model CLIP (Radford et al., 2021), which is based on a pre-trained ViT-B/32 (Dosovitskiy et al., 2021). For LLM QA tasks, we employ Llama-3.1-8B-Instruct (Dubey et al., 2024), Qwen3-32B (Yang et al., 2025), and Llama-3.1-70B-Instruct. For LLM open-ended generation tasks, we use Qwen3-4B-Instruct-2507, Qwen3-4B-Thinking-2507, and DeepSeek-R1-Distill-Qwen-32B (Guo et al., 2025). The specific sampling temperature and other hyperparameters for LLMs are detailed in Appendix F. While the theoretical guarantee of Conformal Labeling is model-agnostic, we show in Appendix I.3 that higher AI model accuracy leads to a larger selection size.

Uncertainty Scores. For the image labeling task, we use the MSP. For the LLM QA task, we also adopt MSP, where the estimated probability of each option is obtained by applying a softmax over the logits corresponding to the option tokens. For the LLM open-ended generation task, we adopt two complementary score functions that serve as analogues of MSP: a logits-based score for the white-box case and a verbalized score for the black-box case. We provide details for these score functions in Appendix E.

Baselines and evaluation metrics. We evaluate Conformal Labeling against four baseline methods: (1) an FDR-search heuristic baseline; (2) selection with guaranteed risk control (SGR) (Geifman & El-Yaniv, 2017); (3) labeling test instances with AI models when the uncertainty score satisfies $S_{n+j} \leq \alpha$; and (4) applying AI predictions to the entire test dataset. We provide a detailed introduction to these baseline methods in Appendix G. We compare Conformal Labeling’s selection procedure against BH (Benjamini & Hochberg, 1995), Storey-BH (Storey, 2002), and Quantile-BH procedures (Benjamini et al., 2006). We evaluate the performance of selective labeling using the following metrics: (1) FDR; (2) Power; (3) AI-labeled ratio, the proportion of data in the test dataset that is labeled by AI models.

Implementation details. Each experiment is repeated 1000 times, and we report the mean FDR, power, and AI-labeled ratio. More details of implementation are provided in Appendix F. We provide the code for reproducing our main experiments in this anonymous repository.

4.2. Results

Conformal Labeling achieves tight FDR control with high power. Table 1 reports the annotation performance of Conformal Labeling on image labeling and LLM QA tasks. Across all the benchmarks and model architectures, Conformal Labeling tightly controls the FDR while labeling a substantial proportion of data with AI models. For example, using Llama-3.1-70B-Instruct on MedMCQA, Conformal Labeling labels 54.83% of test instances with the AI

Table 1. Annotation performance of Conformal Labeling on image Labeling and QA tasks. We compare Conformal Labeling against three baselines: (1) selection with guaranteed risk control (SGR), (2) FDR search heuristic method, and (3) labeling the entire dataset with AI models. We set $\alpha = 0.1$ for Conformal Labeling and FDR search, and $\alpha = 0.1, \epsilon = 0.2$ for SGR. **Bold** numbers are superior results.

Task	Dataset	Model	Conformal Labeling			SGR			FDR search			AI only
			FDR (%)	Power (%)	Ratio (%)	FDR (%)	Power (%)	Ratio (%)	FDR (%)	Power (%)	Ratio (%)	
Image	ImageNet	ResNet-34	9.97	79.89	65.04	8.91	77.31	62.21	9.85	79.63	64.75	26.71
		DenseNet-161	9.92	84.89	72.68	8.92	82.68	70.00	9.83	84.71	72.45	22.89
		CLIP-VIT-B/32	9.84	45.63	30.21	8.17	39.66	25.79	9.77	45.41	30.04	40.35
	ImageNet-V2	ResNet-34	9.92	61.78	41.85	6.69	52.20	34.19	9.78	61.51	41.62	39.04
		DenseNet-161	9.98	67.07	48.57	6.82	54.18	37.98	9.84	66.67	48.21	34.88
		CLIP-VIT-B/32	9.99	35.52	20.73	8.17	6.59	3.67	9.51	33.61	19.55	47.78
QA	MedMCQA	Llama-3.1-8B-Instruct	9.80	31.72	21.20	8.54	2.03	1.27	9.39	30.41	20.27	40.35
		Qwen3-32B	9.81	49.85	37.05	8.08	2.94	2.09	9.55	48.60	36.05	33.44
		Llama-3.1-70B-Instruct	9.86	69.37	54.83	6.43	44.34	33.67	10.58	71.15	56.67	28.90
	MMLU	Llama-3.1-8B-Instruct	9.85	57.13	40.64	7.00	48.00	33.13	58.94	76.77	68.74	35.91
		Qwen3-32B	10.00	82.95	72.44	8.18	78.14	66.88	9.84	82.56	71.98	21.43
		Llama-3.1-70B-Instruct	9.97	88.25	80.17	8.21	84.00	74.85	9.90	88.10	79.98	18.24

Table 2. Annotation performance of Conformal Labeling on open-ended generation tasks. We use the logits-based uncertainty score. We set $\alpha = 0.05$ for Conformal Labeling and FDR search, and $\alpha = 0.05, \epsilon = 0.2$ for SGR. **Bold** numbers indicate superior results.

Dataset	Model	Conformal Labeling			SGR			FDR search			AI only
		FDR (%)	Power (%)	Ratio (%)	FDR (%)	Power (%)	Ratio (%)	FDR (%)	Power (%)	Ratio (%)	
MMLU-Redux	Qwen3-4B-Instruct-2507	4.84	33.62	28.46	43.17	9.06	7.71	4.22	29.87	25.11	20.17
	Qwen3-4B-Thinking-2507	4.95	24.64	21.46	42.56	4.08	3.61	5.85	23.77	20.62	20.79
	DeepSeek-R1-Distill-Qwen-32B	4.92	29.19	26.34	51.35	6.89	6.30	5.80	27.48	24.70	15.07
MATH500	Qwen3-4B-Instruct-2507	4.93	86.73	83.88	3.18	52.83	50.72	4.88	84.94	82.10	8.20
	Qwen3-4B-Thinking-2507	4.07	99.80	99.78	2.50	57.25	57.11	4.01	99.69	99.67	4.00
	DeepSeek-R1-Distill-Qwen-32B	4.18	8.28	8.41	38.70	0.31	0.61	29.83	10.32	10.63	7.00
MATH-L5	Qwen3-4B-Instruct-2507	4.84	69.54	66.90	0.55	2.90	2.85	5.14	68.89	66.25	8.88
	Qwen3-4B-Thinking-2507	4.64	48.33	48.45	0.35	1.96	1.95	4.72	57.85	57.94	5.27
	DeepSeek-R1-Distill-Qwen-32B	4.69	65.31	64.69	1.42	13.86	13.71	6.10	68.66	68.04	6.38
Zebra-Logic	Qwen3-4B-Instruct-2507	4.76	47.80	39.94	0.75	6.52	5.46	4.23	42.36	35.18	20.90
	Qwen3-4B-Thinking-2507	4.95	67.83	63.73	2.45	32.11	30.02	3.05	50.24	46.28	11.00
	DeepSeek-R1-Distill-Qwen-32B	4.78	0.01	0.02	69.33	0.03	0.03	67.70	0.05	0.32	31.40
HumanEval+	Qwen3-4B-Instruct-2507	4.76	72.46	71.06	0.44	5.60	5.38	5.09	81.86	80.08	7.32
	Qwen3-4B-Thinking-2507	2.44	100.00	100.00	1.61	14.73	14.79	2.44	100.00	100.00	2.44
	DeepSeek-R1-Distill-Qwen-32B	0.61	100.00	100.00	0.64	39.48	39.49	0.62	100.00	100.00	0.61

model while controlling the FDR at 9.86%. In comparison, the FDR search baseline fails to control FDR, while SGR only labels 33.67% of test instances. Conformal Labeling improves the AI-labeled ratio by over 20% compared to SGR, while controlling the FDR. The tightest FDR control and highest power are also consistently observed in other datasets and models. Overall, Conformal Labeling achieves the best cost-accuracy tradeoff.

Conformal Labeling outperforms baselines in the open-ended generation task. Table 2 reports the annotation performance of Conformal Labeling on open-ended generation tasks, whereas baselines may incur substantially violated FDR. For example, on MMLU-Redux with Qwen3-4B-Thinking-2507, Conformal Labeling controls the FDR at 4.95% while labeling 21.46% of instances, whereas SGR incurs an FDR of 42.56% and labels only 3.61% of data, and FDR search also exceeds the target FDR with an FDR of 5.85%. Besides,

when baselines control the FDR below the target level, Conformal Labeling consistently achieves higher power than the baselines. Overall, Conformal Labeling achieves the best cost-accuracy tradeoff among all the compared methods.

Logits-based uncertainty score outperforms verbalized uncertainty score in open-ended generation task. Figure 2 compares logits-based and verbalized score functions under varying target level α . Under different score functions, Conformal Labeling consistently controls the FDR below the target level, while using logits-based score function results in higher power. For example, at $\alpha = 0.07$, the logits-based score achieves over 50% power, whereas the verbalized score attains power of approximately 25%, corresponding to an absolute power improvement of over 25%. We also plot the reliability diagrams of these score functions in Figure 6, which shows that logits-based scores achieve lower expected calibration error (ECE) (Naeini et al., 2015) in most datasets, indicating superior reliability. We also plot the p -value distribution under these two score functions in

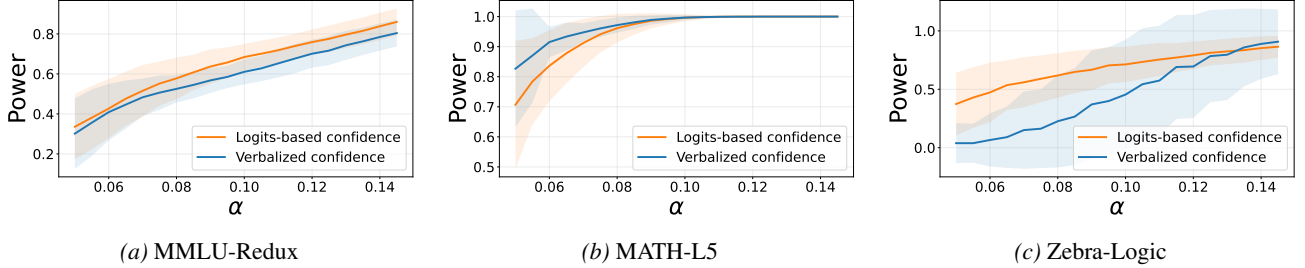


Figure 2. Power of Conformal Labeling with different score functions. The experiments are conducted with Qwen3-4B-Instruct-2507 on three benchmarks. Shaded areas indicate standard deviations. We present the corresponding realized FDR in Figure 5.

Figure 7, which demonstrates that the logits-based uncertainty score provides a clearer separation between incorrect and correct labels. Together, these results demonstrate that the logits-based score provides more reliable uncertainty estimates than the verbalized score, leading to higher power.

Conformal Labeling outperforms existing selection procedures. We conduct an ablation study on the selection procedure by fixing p -values and varying only the selection procedure. We compare Conformal Labeling’s selection procedure with three baselines: Storey-BH (Storey, 2002), Quantile-BH (Benjamini et al., 2006), and the standard BH procedure. Unlike Conformal Labeling that estimates π_0 from the calibration set, Storey-BH and Quantile-BH procedures estimate π_0 from the p -values. We provide a detailed introduction to these procedures in Appendix C. Besides, while Conformal Labeling’s selection procedure requires no hyperparameter tuning, Storey-BH and Quantile-BH involve hyperparameters that must be carefully specified. In this work, we set hyperparameters for these procedures using a bootstrap method (Storey, 2002) detailed in Appendix D.

The comparison results in Table 3 show that our method can achieve much higher power than other selection procedures, with more precise FDR control. For instance, on MATH-L5 with Qwen3-4B-Instruct-2507, Conformal Labeling achieves a power of 94.25% at $\alpha = 0.1$. In comparison, the BH, Storey-BH, and Quantile-BH procedures yield power of 0.09%, 61.42%, and 29.00%, respectively. Conformal Labeling’s selection procedure improves power by over 30% compared to these baselines. The highest power is also consistently observed in other datasets and models. In summary, Conformal Labeling’s selection procedure performs the best among all the compared selection procedures.

How many calibration samples are needed? To study the effect of $|D_{\text{cal}}|$ on FDR and power, in Figure 3, we label $\{5\%, 10\%, 20\%\}$ of the unlabeled dataset as the calibration set. Our results show that Conformal Labeling is robust to calibration set size: even with a 5% calibration ratio, the FDR remains controlled with low standard deviation. Increasing the calibration ratio reduces the variance of both FDR and power, although the improvement from 10% to

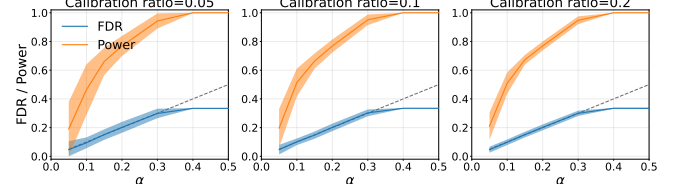


Figure 3. Performance of Conformal Labeling with varying calibration set sizes on MedMCQA with Qwen3-32B. The shaded areas represent standard deviations.

20% is negligible. Based on this trade-off between variance reduction and labeling cost, we use a 10% calibration ratio for image labeling and LLM QA tasks. Overall, while Conformal Labeling is robust to calibration set sizes, larger calibration sets reduce the variance of FDR and power.

Due to space constraints, we defer additional analyses to the appendix. In particular, Appendix I.5 compares our method against FDR search and selective prediction based on calibrated confidence baselines; Appendix I.6 examines whether the selected labels can be used to help train a model with improved accuracy on a synthetic dataset; and Appendix I.7 evaluates Conformal Labeling’s sensitivity to prompt designs in LLM QA tasks.

5. Related work

Conformal Inference. Conformal inference (Vovk et al., 2005; Gazin et al., 2025; Humbert et al., 2025) is a statistical framework characterized by distribution-free and model-agnostic theoretical guarantees. In the literature, two particularly popular directions have emerged: conformal novelty detection (Bates et al., 2023; Bashari et al., 2023; Wu et al., 2025; Bashari et al., 2025; Lee et al., 2025) and conformal selection (Jin & Candès, 2023; Gui et al., 2024). The former focuses on identifying out-of-distribution instances, with recent advances focusing on enhancing selection power by incorporating various forms of side information (Liang et al., 2024; Marandon et al., 2024; Zhao & Sun, 2025). The latter aims to select candidates whose unobserved outcomes exceed user-specified values (Jin & Candès, 2023), which has been extended to multivariate data selection (Bai et al., 2025), online data selection (Xu & Ramdas, 2024; Liu et al.,

Table 3. Comparison of different selection procedures on three labeling tasks. We compare Conformal Labeling’s selection procedure against three baselines: (1) BH procedure, (2) Storey-BH procedure, and (3) Quantile-BH procedure. We report results at $\alpha = 0.1$ for all four selection procedures. **Bold** numbers are superior results.

Task	Dataset	Model	CL		BH		Storey-BH		Quantile BH	
			FDR %	Power %	FDR %	Power (%)	FDR (%)	Power (%)	FDR (%)	Power (%)
Image	ImageNet	ResNet-34	9.97	80.01	2.63	46.85	8.64	74.57	7.57	71.79
		DenseNet-161	9.99	85.03	2.27	44.55	8.34	81.17	7.33	78.40
		CLIP-VIT-B/32	9.98	46.04	4.08	21.70	8.52	41.02	8.05	39.23
	ImageNet-V2	ResNet-34	10.00	61.99	3.84	37.60	9.65	59.84	8.53	57.35
		DenseNet-161	9.83	66.67	3.39	28.39	9.62	65.45	8.44	61.66
		CLIP-VIT-B/32	9.96	34.56	4.85	14.43	9.20	32.25	8.35	28.52
QA	MedMCQA	Llama-3.1-8B-Instruct	9.70	31.44	3.68	12.89	7.43	25.37	6.33	22.11
		Qwen3-32B	9.75	49.80	2.71	10.99	6.99	34.89	6.34	31.27
	MMLU	Llama-3.1-70B-Instruct	9.95	69.67	2.79	29.67	8.48	64.09	6.74	58.06
		Llama-3.1-8B-Instruct	9.99	58.25	3.40	29.49	7.31	49.74	7.17	49.16
		Qwen3-32B	10.00	82.96	1.37	10.51	7.33	74.57	6.25	70.37
	MMLU-Redux	Llama-3.1-70B-Instruct	9.96	88.20	1.61	18.74	6.95	80.08	5.96	76.77
OE	MATH-L5	Qwen3-4B-Instruct-2507	9.96	67.62	1.85	5.52	7.50	50.52	5.15	36.72
		Qwen3-4B-Thinking-2507	9.88	66.37	1.59	1.71	4.93	26.86	3.77	15.58
		DeepSeek-R1-Distill-Qwen-32B	9.84	77.79	1.40	1.80	4.50	29.21	3.44	19.43
	Zebra-Logic	Qwen3-4B-Instruct-2507	10.00	72.70	1.87	4.68	9.45	71.15	6.40	50.41
		Qwen3-4B-Thinking-2507	9.17	93.46	1.16	0.50	6.98	71.90	3.79	45.85
		DeepSeek-R1-Distill-Qwen-32B	8.65	0.14	3.69	0.01	2.80	0.11	3.02	0.01

2025), and human-in-the-loop adaptive data selection (Gu et al., 2025). Besides, some works have developed conformal inference techniques for classification tasks (Zhao & Su, 2023; Sun & Xia, 2025). For example, recent work (Zhao & Su, 2023) proposes controlling the overall error rate in binary and multi-class classification, while a concurrent work (Sun & Xia, 2025) extends this to control the general group-wise false discovery rate within a unified framework. In this work, we motivate and tailor the framework of conformal selection for selective labeling and support the application for open-ended generation tasks.

Selective labeling and prediction. Selective labeling is an increasingly important topic for balancing the tradeoff between labeling cost and error (Gu et al., 2012; Vrabac et al., 2022). While prior work mainly explored heuristic approaches (Li et al., 2023; Duan & Lalor, 2023), a concurrent work (Candès et al., 2025) proposes approximately correct labeling. It guarantees that the overall labeling error is small with high probability by counterbalancing the error of AI labels with the zero error of expert labels. Our work considers a different objective: controlling the labeling error within the AI-labeled subset. Thus, these two methods address different error notions and are applicable in different settings. Notably, our method does not require expert annotations for samples on which the AI model abstains, whereas PAC labeling leverages such annotations to control the overall error. Some other work has also taken steps toward providing statistical guarantees for selective labeling (Zrnic & Candes, 2024; Gligorić et al., 2024), though these works focus on downstream inference rather than guar-

anteeing label quality. Our method is also related to selective prediction, where a model is allowed to abstain from making predictions when uncertain (El-Yaniv & Wiener, 2010; Mozannar & Sontag, 2020; Yang et al., 2023; Kamath et al., 2020; Yoshikawa & Okazaki, 2023). However, most of these methods cannot provide theoretical guarantees on prediction error. While works on selective prediction with risk control (El-Yaniv & Wiener, 2010; Geifman & El-Yaniv, 2017) can provide theoretical guarantees, they target a different error measure called marginal FDR, which is less preferred by prior researchers compared with FDR control. We provide a detailed discussion of the error measures in Appendix I.4.

6. Conclusion

In this paper, we introduce Conformal Labeling, a novel method for identifying a subset where AI predictions can be provably trusted. Specifically, we construct conformal p -values and estimate the accuracy of AI models using a small labeled calibration dataset. Then, we design a principled selection procedure that automatically adapts to the estimated accuracy, with higher accuracy permitting a larger threshold. We provide theoretical guarantees that Conformal Labeling controls the FDR below the nominal level under mild assumptions. Extensive experiments demonstrate that Conformal Labeling achieves tight FDR control and high power across various tasks, including image labeling, LLM QA, and LLM open-ended generation tasks. We hope that the insights from this work will inspire future research on rigorous methods for selective labeling.

References

Bai, T., Zhao, Y., Yu, X., and Yang, A. Y. Multivariate conformal selection. In *Forty-second International Conference on Machine Learning*, 2025. URL <https://openreview.net/forum?id=g2tr7nA4pS>.

Bashari, M., Epstein, A., Romano, Y., and Sesia, M. Derandomized novelty detection with fdr control via conformal e-values. *Advances in Neural Information Processing Systems*, 36:65585–65596, 2023.

Bashari, M., Sesia, M., and Romano, Y. Robust conformal outlier detection under contaminated reference data. In *Forty-second International Conference on Machine Learning*, 2025. URL <https://openreview.net/forum?id=s55Af9Emyq>.

Bates, S., Candès, E., Lei, L., Romano, Y., and Sesia, M. Testing for outliers with conformal p-values. *The Annals of Statistics*, 51(1):149–178, 2023.

Baumann, J., Röttger, P., Urman, A., Wendsjö, A., del Arco, F. M. P., Gruber, J. B., and Hovy, D. Large language model hacking: Quantifying the hidden risks of using llms for text annotation, 2025. URL <https://arxiv.org/abs/2509.08825>.

Benjamini, Y. and Hochberg, Y. Controlling the false discovery rate: a practical and powerful approach to multiple testing. *Journal of the Royal statistical society: series B (Methodological)*, 57(1):289–300, 1995.

Benjamini, Y. and Yekutieli, D. The control of the false discovery rate in multiple testing under dependency. *The Annals of Statistics*, 29(4):1165–1188, 2001.

Benjamini, Y., Krieger, A. M., and Yekutieli, D. Adaptive linear step-up procedures that control the false discovery rate. *Biometrika*, 93(3):491–507, 2006.

Bernhardt, M., Castro, D. C., Tanno, R., Schwaighofer, A., Tezcan, K. C., Monteiro, M., Bannur, S., Lungren, M. P., Nori, A., Glocker, B., et al. Active label cleaning for improved dataset quality under resource constraints. *Nature communications*, 13(1):1161, 2022.

Candès, E. J., Ilyas, A., and Zrnic, T. Probably approximately correct labels. *arXiv preprint arXiv:2506.10908*, 2025. URL <https://arxiv.org/abs/2506.10908>.

Chhikara, P. Mind the confidence gap: Overconfidence, calibration, and distractor effects in large language models. *arXiv preprint arXiv:2502.11028*, 2025.

Deng, J., Dong, W., Socher, R., Li, L.-J., Li, K., and Fei-Fei, L. Imagenet: A large-scale hierarchical image database. In *2009 IEEE Conference on Computer Vision and Pattern Recognition*, pp. 248–255, 2009. doi: 10.1109/CVPR.2009.5206848.

Dosovitskiy, A., Beyer, L., Kolesnikov, A., Weissenborn, D., Zhai, X., Unterthiner, T., Dehghani, M., Minderer, M., Heigold, G., Gelly, S., Uszkoreit, J., and Houlsby, N. An image is worth 16x16 words: Transformers for image recognition at scale. In *International Conference on Learning Representations*, 2021. URL <https://openreview.net/forum?id=YicbFdNTTy>.

Duan, X. and Lalor, J. P. H-coal: Human correction of ai-generated labels for biomedical named entity recognition. *arXiv preprint arXiv:2311.11981*, 2023.

Dubey, A., Jauhri, A., Pandey, A., Kadian, A., Al-Dahle, A., Letman, A., Mathur, A., Schelten, A., Yang, A., Fan, A., et al. The llama 3 herd of models. *arXiv e-prints*, pp. arXiv–2407, 2024.

El-Yaniv, R. and Wiener, Y. On the foundations of noise-free selective classification. *Journal of Machine Learning Research*, 11(53):1605–1641, 2010. URL <http://jmlr.org/papers/v11/el-yaniv10a.html>.

Gazin, U., Heller, R., Marandon, A., and Roquain, E. Selecting informative conformal prediction sets with false coverage rate control. *Journal of the Royal Statistical Society Series B: Statistical Methodology*, pp. qkae120, 2025.

Geifman, Y. and El-Yaniv, R. Selective classification for deep neural networks. *Advances in Neural Information Processing Systems*, 30, 2017.

Gema, A. P., Leang, J. O. J., Hong, G., Devoto, A., Mancino, A. C. M., Saxena, R., He, X., Zhao, Y., Du, X., Madani, M. R. G., et al. Are we done with mmlu? In *Proceedings of the 2025 Conference of the Nations of the Americas Chapter of the Association for Computational Linguistics: Human Language Technologies (Volume 1: Long Papers)*, pp. 5069–5096, 2025.

Gligorić, K., Zrnic, T., Lee, C., Candès, E. J., and Jurafsky, D. Can unconfident llm annotations be used for confident conclusions? *arXiv preprint arXiv:2408.15204*, 2024.

Granese, F., Romanelli, M., Gorla, D., Palamidessi, C., and Piantanida, P. Doctor: A simple method for detecting misclassification errors. *Advances in Neural Information Processing Systems*, 34:5669–5681, 2021.

Gu, Q., Zhang, T., Han, J., and Ding, C. Selective labeling via error bound minimization. *Advances in Neural Information Processing Systems*, 25, 2012.

Gui, Y., Jin, Y., and Ren, Z. Conformal alignment: Knowing when to trust foundation models with guarantees. *Advances in Neural Information Processing Systems*, 37: 73884–73919, 2024.

Gui, Y., Jin, Y., Nair, Y., and Ren, Z. Acs: An interactive framework for conformal selection. *arXiv preprint arXiv:2507.15825*, 2025.

Guo, C., Pleiss, G., Sun, Y., and Weinberger, K. Q. On calibration of modern neural networks. In *International Conference on Machine Learning*, pp. 1321–1330. PMLR, 2017.

Guo, D., Yang, D., Zhang, H., Song, J., Zhang, R., Xu, R., Zhu, Q., Ma, S., Wang, P., Bi, X., et al. Deepseek-r1: Incentivizing reasoning capability in llms via reinforcement learning. *arXiv preprint arXiv:2501.12948*, 2025.

He, K., Zhang, X., Ren, S., and Sun, J. Deep residual learning for image recognition. In *Proceedings of the IEEE conference on computer vision and pattern recognition*, pp. 770–778, 2016.

Hendrycks, D. and Gimpel, K. A baseline for detecting misclassified and out-of-distribution examples in neural networks. *arXiv preprint arXiv:1610.02136*, 2016.

Hendrycks, D., Burns, C., Basart, S., Zou, A., Mazeika, M., Song, D., and Steinhardt, J. Measuring massive multitask language understanding. In *International Conference on Learning Representations (ICLR)*, 2021. arXiv:2009.03300.

Huang, G., Liu, Z., van der Maaten, L., and Weinberger, K. Q. Densely connected convolutional networks, 2018. URL <https://arxiv.org/abs/1608.06993>.

Humbert, P., Gazin, U., Heller, R., and Roquain, E. Online selective conformal inference: adaptive scores, convergence rate and optimality. *arXiv preprint arXiv:2508.10336*, 2025.

Jin, Y. and Candès, E. J. Selection by prediction with conformal p-values. *Journal of Machine Learning Research*, 24(244):1–41, 2023.

Jin, Y. and Candès, E. J. Model-free selective inference under covariate shift via weighted conformal p-values. *Biometrika*, pp. asaf066, 2025.

Kamath, A., Jia, R., and Liang, P. Selective question answering under domain shift. *arXiv preprint arXiv:2006.09462*, 2020.

Lee, J., Popov, I., and Ren, Z. Full-conformal novelty detection: A powerful and non-random approach. *arXiv preprint arXiv:2501.02703*, 2025.

Li, M., Shi, T., Ziems, C., Kan, M.-Y., Chen, N., Liu, Z., and Yang, D. Coannotating: Uncertainty-guided work allocation between human and large language models for data annotation. In *Proceedings of the 2023 Conference on Empirical Methods in Natural Language Processing*. Association for Computational Linguistics, 2023. doi: 10.18653/v1/2023.emnlp-main.92. URL <http://dx.doi.org/10.18653/v1/2023.emnlp-main.92>.

Liang, Z., Sesia, M., and Sun, W. Integrative conformal p-values for out-of-distribution testing with labelled outliers. *Journal of the Royal Statistical Society Series B: Statistical Methodology*, 86(3):671–693, 01 2024. ISSN 1369-7412. doi: 10.1093/rssb/qkad138. URL <https://doi.org/10.1093/rssb/qkad138>.

Lightman, H., Kosaraju, V., Burda, Y., Edwards, H., Baker, B., Lee, T., Leike, J., Schulman, J., Sutskever, I., and Cobbe, K. Let’s verify step by step. In *The Twelfth International Conference on Learning Representations*, 2023.

Lin, B. Y., Bras, R. L., Richardson, K., Sabharwal, A., Poovendran, R., Clark, P., and Choi, Y. ZebraLogic: On the scaling limits of LLMs for logical reasoning. In *Forty-second International Conference on Machine Learning*, 2025. URL <https://openreview.net/forum?id=sTAJ9QyA61>.

Liu, J., Xia, C. S., Wang, Y., and Zhang, L. Is your code generated by chatgpt really correct? rigorous evaluation of large language models for code generation. *Advances in Neural Information Processing Systems*, 36:21558–21572, 2023.

Liu, K., Xi, H., Vong, C.-M., and Wei, H. Online conformal selection with accept-to-reject changes. *arXiv preprint arXiv:2508.13838*, 2025.

Liu, W., Wang, X., Owens, J., and Li, Y. Energy-based out-of-distribution detection. *Advances in Neural Information Processing Systems*, 33:21464–21475, 2020.

Luo, B., Wang, S., Li, S., and Wei, H. Your pre-trained LLM is secretly an unsupervised confidence calibrator. In *The Thirty-ninth Annual Conference on Neural Information Processing Systems*, 2025. URL <https://openreview.net/forum?id=I4PJYZvfW5>.

Marandon, A., Lei, L., Mary, D., and Roquain, E. Adaptive novelty detection with false discovery rate guarantee. *The Annals of Statistics*, 52(1):157–183, 2024.

Mozannar, H. and Sontag, D. Consistent estimators for learning to defer to an expert. In *International Conference on Machine Learning*, pp. 7076–7087. PMLR, 2020.

Naeini, M. P., Cooper, G., and Hauskrecht, M. Obtaining well calibrated probabilities using bayesian binning. In *Proceedings of the AAAI conference on artificial intelligence*, volume 29, 2015.

Northcutt, C. G., Athalye, A., and Mueller, J. Pervasive label errors in test sets destabilize machine learning benchmarks, 2021. URL <https://arxiv.org/abs/2103.14749>.

Pal, A., Umapathi, L. K., and Sankarasubbu, M. Medmcqa : A large-scale multi-subject multi-choice dataset for medical domain question answering, 2022. URL <https://arxiv.org/abs/2203.14371>.

Radford, A., Kim, J. W., Hallacy, C., Ramesh, A., Goh, G., Agarwal, S., Sastry, G., Askell, A., Mishkin, P., Clark, J., Krueger, G., and Sutskever, I. Learning transferable visual models from natural language supervision, 2021. URL <https://arxiv.org/abs/2103.00020>.

Recht, B., Roelofs, R., Schmidt, L., and Shankar, V. Do imangenet classifiers generalize to imangenet?, 2019. URL <https://arxiv.org/abs/1902.10811>.

Storey, J. D. A direct approach to false discovery rates. *Journal of the Royal Statistical Society Series B: Statistical Methodology*, 64(3):479–498, 2002.

Storey, J. D. The positive false discovery rate: a bayesian interpretation and the q-value. *The annals of statistics*, 31(6):2013–2035, 2003.

Sun, Y. and Xia, Y. A unified framework for large-scale classification: Error rate control and optimality. *arXiv preprint arXiv:2504.07321*, 2025.

Tan, Z., Li, D., Wang, S., Beigi, A., Jiang, B., Bhattacharjee, A., Karami, M., Li, J., Cheng, L., and Liu, H. Large language models for data annotation and synthesis: A survey. *arXiv preprint arXiv:2402.13446*, 2024.

Tu, W., Deng, W., Zheng, L., and Gedeon, T. What does softmax probability tell us about classifiers ranking across diverse test conditions? *arXiv preprint arXiv:2406.09908*, 2024.

Vovk, V., Gammerman, A., and Saunders, C. Machine-learning applications of algorithmic randomness. 1999.

Vovk, V., Gammerman, A., and Shafer, G. *Algorithmic learning in a random world*. Springer, 2005.

Vrabac, D., Smit, A., He, Y., Ng, A. Y., Beam, A. L., and Rajpurkar, P. Medselect: Selective labeling for medical image classification using meta-learning. In *International Conference on Medical Imaging with Deep Learning*, pp. 1301–1310. PMLR, 2022.

Wang, H., Jin, Q., Li, S., Liu, S., Wang, M., and Song, Z. A comprehensive survey on deep active learning in medical image analysis. *Medical Image Analysis*, 95: 103201, 2024a.

Wang, S., Liu, Y., Xu, Y., Zhu, C., and Zeng, M. Want to reduce labeling cost? gpt-3 can help. *arXiv preprint arXiv:2108.13487*, 2021.

Wang, X., Lian, L., and Yu, S. X. Unsupervised selective labeling for more effective semi-supervised learning, 2023. URL <https://arxiv.org/abs/2110.03006>.

Wang, X., Kim, H., Rahman, S., Mitra, K., and Miao, Z. Human-llm collaborative annotation through effective verification of llm labels. In *Proceedings of the 2024 CHI Conference on Human Factors in Computing Systems*, pp. 1–21, 2024b.

Wang, Y., Ma, X., Zhang, G., Ni, Y., Chandra, A., Guo, S., Ren, W., Arulraj, A., He, X., Jiang, Z., et al. Mmlu-pro: A more robust and challenging multi-task language understanding benchmark. *arXiv preprint arXiv:2406.01574*, 2024c.

Wu, X., Lu, L., Wang, Z., and Zou, C. Conditional testing based on localized conformal Sp\$-values. In *The Thirteenth International Conference on Learning Representations*, 2025. URL <https://openreview.net/forum?id=Ip6UwB35uT>.

Xiao, R., Dong, Y., Zhao, J., Wu, R., Lin, M., Chen, G., and Wang, H. Freeal: Towards human-free active learning in the era of large language models. *arXiv preprint arXiv:2311.15614*, 2023.

Xu, Z. and Ramdas, A. Online multiple testing with e-values. In *International Conference on Artificial Intelligence and Statistics*, pp. 3997–4005. PMLR, 2024.

Yang, A., Li, A., Yang, B., Zhang, B., Hui, B., Zheng, B., Yu, B., Gao, C., Huang, C., Lv, C., Zheng, C., Liu, D., Zhou, F., Huang, F., Hu, F., Ge, H., Wei, H., Lin, H., Tang, J., Yang, J., Tu, J., Zhang, J., Yang, J., Yang, J., Zhou, J., Zhou, J., Lin, J., Dang, K., Bao, K., Yang, K., Yu, L., Deng, L., Li, M., Xue, M., Li, M., Zhang, P., Wang, P., Zhu, Q., Men, R., Gao, R., Liu, S., Luo, S., Li, T., Tang, T., Yin, W., Ren, X., Wang, X., Zhang, X., Ren, X., Fan, Y., Su, Y., Zhang, Y., Zhang, Y., Wan, Y., Liu, Y., Wang, Z., Cui, Z., Zhang, Z., Zhou, Z., and Qiu, Z. Qwen3 technical report, 2025. URL <https://arxiv.org/abs/2505.09388>.

Yang, Q., Ravikumar, S., Schmitt-Ulms, F., Lolla, S., Demir, E., Elistratov, I., Lavaee, A., Lolla, S., Ahmadi, E., Rus, D., et al. Uncertainty-aware language modeling for selective question answering. *arXiv preprint arXiv:2311.15451*, 2023.

Yoshikawa, H. and Okazaki, N. Selective-lama: Selective prediction for confidence-aware evaluation of language models. In *Findings of the Association for Computational Linguistics: EACL 2023*, pp. 2017–2028, 2023.

Zhao, G. and Su, Z. Controlling f_{SR} in selective classification. *arXiv preprint arXiv:2311.03811*, 2023.

Zhao, Z. and Sun, W. A conformalized empirical bayes method for multiple testing with side information, 2025. URL <https://arxiv.org/abs/2502.19667>.

Zrnic, T. and Candes, E. Active statistical inference. In *Forty-first International Conference on Machine Learning*, 2024. URL <https://openreview.net/forum?id=GKMCCtWC7H>.

A. Technical proofs

A.1. Lemmas for proving Theorem 3.2

Lemma A.1. (Benjamini & Yekutieli (2001), Theorem 1.2) *If the joint distribution of the p-values is PRDS on the subset corresponding to true null hypotheses, applying the Benjamini–Hochberg procedure at level α guarantees*

$$FDR \leq \frac{m_0}{m} \alpha,$$

where m_0 is the number of true null hypotheses.

Lemma A.2. *Under the assumptions of Theorem 3.2, where the calibration samples $(X_i, Y_i)_{i=1}^n$ and the test samples $(X_{n+j}, Y_{n+j})_{j=1}^m$ are independently and identically distributed (i.i.d.), and conditional on n_0 (the number of true null hypotheses in the calibration set) and m_0 (the number of true null hypotheses in the test set), the expected false discovery proportion (FDP) satisfies*

$$\mathbb{E}[FDP \mid n_0, m_0] \leq \frac{1+n}{1+n_0} \frac{m_0}{m} \alpha,$$

where $\alpha \in (0, 1)$ is the target false discovery rate (FDR) level, and the selection set \mathcal{R} is determined by Algorithm 1.

Proof. Without loss of generality, assume that the first n_0 calibration samples and the first m_0 test samples correspond to true null hypotheses. By the standard result in conformal inference (Vovk et al., 2005) we have,

$$P(\hat{p}_{n+j} \leq t \mid n_0, m_0) \leq t \quad \text{for all } t \in [0, 1], \quad j = 1, \dots, m_0.$$

From results in (Bates et al., 2023), we know conformal p-values $(\hat{p}_1, \dots, \hat{p}_m)$ are PRDS on the set of mislabeled data. Lemma A.1 hence guarantees that conditional on n_0 and m_0 , applying Conformal Labeling at level α satisfies

$$\mathbb{E}[FDP \mid n_0, m_0] \leq \frac{1+n}{1+n_0} \frac{m_0}{m} \alpha,$$

□

A.2. Proof of theorem 3.2

Proof of theorem 3.2. Under the i.i.d. assumption of Theorem 3.2, the calibration samples $(X_i, Y_i)_{i=1}^n$ and the test samples $(X_{n+j}, Y_{n+j})_{j=1}^m$ are independently and identically distributed. This implies that each hypothesis, whether from the calibration or test set, has an equal probability p of being a true null, where p represents the expected probability of incorrect prediction under the null hypothesis.

Consequently, the number of true null hypotheses in the calibration set, denoted n_0 , follows a binomial distribution $n_0 \sim \text{Binomial}(n, p)$, and the number of true null hypotheses in the test set, denoted m_0 , follows $m_0 \sim \text{Binomial}(m, p)$. The independence across the calibration and test sets arises from the i.i.d. structure, ensuring that n_0 and m_0 are independent random variables.

Using the law of total expectation, we express FDR as

$$\begin{aligned} \text{FDR} &= \mathbb{E}[\text{FDP}] \\ &= \mathbb{E}[\mathbb{E}[\text{FDP} \mid n_0, m_0]] \\ &\leq \mathbb{E}\left[\frac{m_0}{m} \frac{1+n}{1+n_0} \alpha\right] \quad \text{by Lemma A.2} \\ &= \mathbb{E}\left[\frac{m_0}{m}\right] \cdot \mathbb{E}\left[\frac{1+n}{1+n_0}\right] \cdot \alpha \quad \text{since } n_0 \text{ and } m_0 \text{ are independent} \\ &= p \cdot \mathbb{E}\left[\frac{1+n}{1+n_0}\right] \cdot \alpha \quad \text{since } m_0 \sim \text{Binomial}(m, p) \end{aligned} \tag{6}$$

Now it suffices to show that $p \cdot \mathbb{E}\left[\frac{1+n}{1+n_0}\right] = [1 - (1-p)^{n+1}]$.

Since n_0 has probability mass function

$$\mathbb{P}(n_0 = k) = \binom{n}{k} p^k (1-p)^{n-k}, \quad k = 0, 1, \dots, n,$$

we compute

$$\begin{aligned}
 p \cdot \mathbb{E} \left[\frac{1+n}{1+k} \right] &= p \cdot \sum_{k=0}^n \frac{1+n}{1+k} \binom{n}{k} p^k (1-p)^{n-k} \\
 &= \sum_{k=0}^n \frac{(n+1)!}{(k+1)!(n-k)!} p^{k+1} (1-p)^{n-k} \\
 &= \sum_{k=0}^n \binom{n+1}{k+1} p^{k+1} (1-p)^{n-k} \\
 &= \sum_{l=1}^{n+1} \binom{n+1}{l} p^l (1-p)^{n+1-l} \quad \text{by letting } l = k+1 \\
 &= \sum_{l=0}^{n+1} \binom{n+1}{l} p^l (1-p)^{n+1-l} - \binom{n+1}{0} p^0 (1-p)^{n+1-0} \\
 &= \sum_{l=0}^{n+1} \mathbb{P}(X = l) - (1-p)^{n+1} \quad \text{where } X \sim \text{Binomial}(n+1, p) \\
 &= 1 - (1-p)^{n+1}
 \end{aligned} \tag{7}$$

This completes the proof, establishing the desired bound on the FDR. □

B. Overview of Different Uncertainty Score Functions

In this section, we provide an overview of three representative uncertainty score functions that are widely used in misclassification detection: Maximum Softmax Probability (MSP) (Hendrycks & Gimpel, 2016), the energy-based score (Liu et al., 2020), and the DOCTOR- α score (Granese et al., 2021). Each of these functions captures predictive uncertainty from a different perspective.

Maximum Softmax Probability (MSP). The Maximum Softmax Probability (MSP) baseline (Hendrycks & Gimpel, 2016) proposes to use confidence of the AI model as an uncertainty score.

$$S_{\text{MSP}}(x) = 1 - \max_{y \in \mathcal{Y}} p_y(x),$$

where $p_y(x)$ is the softmax probability assigned to class y for input x . The key idea is straightforward: if the model assigns a high probability to its most likely class, the prediction is considered confident. Although MSP is simple and effective, it has notable limitations: it only reflects the confidence in the top-1 prediction and ignores the structure of the remaining probability distribution, which may contain useful information about uncertainty.

Energy-based score. The energy-based score (Liu et al., 2020) is defined as

$$S_{\text{Energy}}(x) = \log \sum_{y \in \mathcal{Y}} \exp(f_y(x)),$$

where $f_y(x)$ denotes the logit value for class y and $T > 0$ is a temperature parameter. This score is derived from the concept of energy in statistical physics and leverages the log-sum-exp operator over all logits. Unlike MSP, which only considers the maximum probability, the energy score integrates information from the full logit vector, thereby providing a smoother and more informative confidence measure.

DOCTOR- α score. The DOCTOR- α score (Granese et al., 2021) is defined as

$$S_\alpha(x) = \sum_{y \in \mathcal{Y}} p_y(x)^2,$$

where $p_y(x)$ denotes the softmax probability for class y . This score is inspired by information-theoretic measures of uncertainty, as it is closely related to the quadratic Rényi entropy. The intuition is that if the predictive distribution is sharp (i.e., one class has probability close to one), then $\sum_y p_y(x)^2$ will be large, indicating high confidence. Conversely, if the distribution is flat (i.e., the model is uncertain and spreads probability mass across many classes), then $S_\alpha(x)$ will be small. Compared to MSP, the DOCTOR- α score leverages information from the entire probability distribution rather than only the top prediction, making it a richer measure of uncertainty for misclassification detection.

C. BH Procedure and its Adaptive Variants

Consider testing m null hypotheses H_0^1, \dots, H_0^m based on their corresponding p -values $\{p_1, p_2, \dots, p_m\}$. For a true null hypothesis H_0^j , the corresponding p -value p_j is a random variable that is super-uniform on $[0, 1]$ under the null hypothesis. Formally, for any $u \in [0, 1]$,

$$\mathbb{P}(p_j \leq u \mid H_0^j \text{ is true}) \leq u.$$

Define $p_{(j)}$ as the j -th smallest p -value among a set of p -values $\{p_1, p_2, \dots, p_m\}$. Given a set of p -values $\{p_1, p_2, \dots, p_m\}$, the BH algorithm returns $S = \{j \in \{0, \dots, m\} : p_{(j)} \leq \frac{\alpha j^*}{m}\}$, where α is the target FDR level and

$$j^* = \max\{j \in \{1, \dots, m\} : p_{(j)} \leq \frac{\alpha j}{m}\}$$

When the null p -values $\{p_j : j \in \mathcal{H}_0\}$ are independent, the BH procedure is proved to control the FDR at level $\pi_0 \alpha$ in finite samples (Benjamini & Hochberg, 1995), where $\pi_0 = \frac{|\mathcal{H}_0|}{m}$ is the proportion of true nulls. The independence assumption can be further relaxed to the PRDS condition (Benjamini & Yekutieli, 2001).

If π_0 is small, the FDR control will be overly conservative. For example, if a classifier achieves a 80% accuracy in the unlabeled test dataset, then $\pi_0 = 0.2$ —which leads to overly conservative FDR control. When π_0 is known, we can apply BH procedure at level $\frac{\alpha}{\pi_0}$ to close the gap. In practice, π_0 is typically unknown. Several adaptive BH procedures attempt to address this issue by estimating π_0 and adjusting the target FDR level α accordingly. These procedures are often called the π_0 -adaptive versions of the BH algorithm. Two most famous estimators are Storey-BH (Storey, 2002) and Quantile-BH (Benjamini et al., 2006):

$$\begin{aligned} \hat{\pi}_0^{Storey}(\lambda) &= \frac{1 + \sum_{i=1}^m \mathbf{1}\{p_i \geq \lambda\}}{m(1 - \lambda)}, \lambda \in (0, 1) \\ \hat{\pi}_0^{Quant}(k_0) &= \frac{m - k_0 + 1}{m(1 - p_{(k_0)})}, k_0 \in \{1, \dots, m\} \end{aligned}$$

λ and k_0 are hyperparameters determined by users.

D. Hyperparameter selection for BH adaptive variants

Both Storey-BH and Quant-BH require careful hyperparameter selection— λ for Storey-BH and k_0 for Quant-BH—as this choice significantly impacts their performance. Following Storey (2002), we employ a bootstrap-based method to select the optimal λ (and analogously, k_0 for the Quantile BH procedure). Further details can be found in Section 9 of Storey (2002). The algorithm proceeds as follows:

1. Define a grid R for the hyperparameter, i.e. $R = \{0.1, 0.2, \dots, 0.9\}$ for Storey-BH.
2. For each $\lambda \in R$, compute:

$$\widehat{\text{pFDR}}_\lambda(\gamma) = \frac{\hat{\pi}_0(\lambda)\gamma}{\widehat{\Pr}(p \leq \gamma)\{1 - (1 - \gamma)^m\}} \quad (8)$$

Table 4. Prompt for the verbalized confidence scores.

System prompt: You are a reasoning assistant. For each question and proposed answer, you must estimate how likely the proposed answer is correct.

User prompt:

Question: {QUESTION}

Answer: {ANSWER}

Provide a probability (between 0.0 and 1.0) that your answer is correct. Only output the probability.

where $\widehat{\pi}_0(\lambda) = \widehat{\pi}_0^{Storey}(\lambda)$ or $\widehat{\pi}_0^{Quant}(\lambda)$ and $\widehat{\Pr}(p \leq \gamma)$ is the empirical estimate of $\Pr(p \leq \gamma)$

3. Generate B bootstrap replicates $\{p_1^{*,b}, \dots, p_m^{*,b}\}_{b=1}^B$ and compute $\widehat{\text{pFDR}}_{\lambda}^{*,b}(\gamma)$ for each b .
4. Estimate the MSE for each λ :

$$\widehat{\text{MSE}}(\lambda) = \frac{1}{B} \sum_{b=1}^B \left(\widehat{\text{pFDR}}_{\lambda}^{*,b}(\gamma) - \min_{\lambda' \in R} \widehat{\text{pFDR}}_{\lambda'}(\gamma) \right)^2 \quad (9)$$

5. Select $\widehat{\lambda} = \operatorname{argmin}_{\lambda \in R} \widehat{\text{MSE}}(\lambda)$

E. Uncertainty score functions for open-ended generation task

Logits-based uncertainty score. In particular, let $y = (y_1, y_2, \dots, y_l)$ be a generated sequence of length l . We define the logits-based score as:

$$S_{\text{logits}}(x) = 1 - \frac{1}{l} \sum_{j=1}^l \mathbb{P}(y_j \mid y_1, \dots, y_{j-1}, x)$$

where $\mathbb{P}(y_j \mid y_1, \dots, y_{j-1}, x)$ is the conditional probability of token y_j . This score measures the average confidence of the model across all generated tokens. When the model is very confident about each token, the score is low. When the model is less confident, the score is high, indicating an example that may benefit from a more capable annotation source.

Verbalized uncertainty score For the verbalized score, we first let the model explicitly state its self-reported confidence. The uncertainty score is then defined as one minus the self-reported confidence. In this work, we report the average confidence over 10 trials, and the prompts are listed in Table 4.

F. Implementation details

Hyperparameter settings of LLMs For the open-ended generation task, we configure the decoding parameters as follows. For Qwen/Qwen3-4B-Instruct-2507, we set Temperature=0.7, TopP=0.8, TopK=20, and MinP=0. For Qwen/Qwen3-4B-Thinking-2507, we set Temperature=0.6, TopP=0.95, TopK=20, and MinP=0. For DeepSeek/DeepSeek-R1-Distill-Qwen-32B, we set Temperature=0.6, TopP=0.95, and MinP=0. All experiments were run on NVIDIA GeForce RTX 4090, NVIDIA L40, and NVIDIA RTX Pro 6000.

Dataset splitting strategy. For image labeling and LLM QA tasks, we randomly split 10% of the unlabeled dataset as the calibration dataset. For open-ended generation task, we use dataset-specific splitting strategy, which is detailed in Table ??.

Prompts for LLM QA task We adopt the same prompts as in Luo et al. (2025). The prompt is presented in Table 6.

G. Compared baselines

We compare Conformal Labeling against four baseline methods: (1) an FDR-search heuristic baseline; (2) selection with guaranteed risk control (SGR) (Geifman & El-Yaniv, 2017); (3) labeling test instances with AI models when the uncertainty

Table 5. Details of dataset splitting settings for open-ended generation task.

Dataset	Dataset Type	Dataset Size	Split Setting	Size
MMLU-Redux	General Task	3000	Calibration Test	500 2500
MATH-500	Math Reasoning	500	Calibration Test	300 200
MATH-L5	Math Reasoning	721	Calibration Test	300 421
Zebra-Logic	Text Reasoning	750	Calibration Test	300 450
HumanEval+	Coding Task	164	Calibration Test	100 64

Table 6. Prompt for LLM QA task

Dataset	Prompt
LLM QA	The following are multiple-choice questions. Give ONLY the correct option, no other words or explanation: [Question] A: [Option 1] B: [Option 2] C: [Option 3] D: [Option 4] Answer: [Mask]

score satisfies $\mathcal{S}_{n+j} \leq \alpha$; and (4) applying AI predictions to the entire test dataset. FDR-search heuristic baseline selects the largest uncertainty threshold such that the empirical FDR of the calibration dataset does not surpass α . SGR is a theoretically rigorous method that provides high-probability guarantees on marginal FDR control. It searches for the cutoff over a grid of confidence values, and then takes a union bound to achieve the overall error control. We provide a detailed introduction to the FDR-search heuristic baseline and SGR below.

FDR-search heuristic baseline. Let $S(X)$ be a confidence function such as MSP. For a confidence threshold t , we define the empirical FDR on the calibration set as

$$\widehat{\text{FDR}}(t) = \frac{\sum_{i=1}^n \mathbf{1}\{S(x_i) \geq t, Y_i \neq \widehat{Y}_i\}}{\max\{\sum_{i=1}^n \mathbf{1}\{S(x_i) \geq t\}, 1\}}$$

The threshold is selected by searching from the largest to the smallest confidence value. Specifically, we start from the smallest possible threshold and progressively increase t until the empirical FDR on the calibration set falls below the target level α :

$$t^*(\alpha) = \min\{t : \widehat{\text{FDR}}_{\text{cal}}(t) \leq \alpha\}.$$

Then a test instance is selected if its uncertainty score satisfies $\mathcal{S}(X_i) \geq t^*(\alpha)$.

Selection with guaranteed risk control (SGR). Let f be a fixed classifier and let $c : \mathcal{X} \rightarrow \mathbb{R}$ be a confidence score, where larger values indicate more reliable predictions. For a threshold θ , define the selection rule

$$g_\theta(x) = \mathbf{1}\{c(x) \geq \theta\},$$

so that predictions are made only on instances with confidence at least θ . For a calibration set $\{(x_i, y_i)\}_{i=1}^n$, the empirical selective risk at threshold θ is

$$\widehat{R}(\theta) = \frac{\sum_{i=1}^n \mathbf{1}\{g_\theta(x_i) = 1, f(x_i) \neq y_i\}}{\max\{\sum_{i=1}^n \mathbf{1}\{g_\theta(x_i) = 1\}, 1\}}.$$

The SGR algorithm searches over candidate thresholds (ordered from high to low confidence) and, for each threshold, computes a high-probability upper bound on the true selective risk based on the calibration data. The output threshold θ^* is the largest threshold whose risk bound does not exceed a target level r^* . At test time, an instance is selected if $c(X_i) \geq \theta^*$.

Algorithm 2 Conformal Labeling for Regression Tasks

Input: Calibration set $\mathcal{D}_{\text{cal}} = \{(X_i, Y_i)\}_{i=1}^n$; test instances $\{X_{n+j}\}_{j=1}^m$; pre-trained predictor f ; loss function L ; loss threshold ϵ ; target FDR level $\alpha \in (0, 1)$; nonconformity scores $\{S_i\}_{i=1}^{n+m}$

Output: Selected set \mathcal{S} with FDR control

- 1: // Step 0: Identify calibration samples exceeding the loss threshold
- 2: Set $\mathcal{D}_{\text{cal}}^0 = \{(X_i, Y_i) : L(Y_i, \hat{Y}_i) > \epsilon\}_{i=1}^n$, and let $n_0 = |\mathcal{D}_{\text{cal}}^0|$.
- 3: // Step 1: Construct conformal p-values
- 4: **for** $j = 1$ to m **do**
- 5: Compute the conformal p-value \hat{p}_j according to Eq. (3).
- 6: **end for**
- 7: // Step 2: Step-up thresholding
- 8: Compute $j^* = \max \left\{ j : \hat{p}_{(j)} \leq \frac{\alpha j(n+1)}{m(n_0+1)} \right\}$, where $\hat{p}_{(j)}$ is the j -th smallest p-value.
- 9: **Return** $\mathcal{S} = \{j : \hat{p}_j \leq \hat{p}_{(j^*)}\}$.

Theorem G.1 (Selective risk guarantee of SGR). *Fix a target risk level $\alpha \in (0, 1)$ and a confidence parameter $\delta \in (0, 1)$. Let θ^* be the threshold returned by the SGR algorithm using a calibration set of size n . Then, with probability at least $1 - \delta$ over the draw of the calibration set, the resulting selective classifier (f, g_{θ^*}) satisfies*

$$R(f, g_{\theta^*}) \leq \alpha,$$

where $R(f, g_{\theta^*})$ denotes the true selective risk.

In the labeling task, the risk function is defined as

$$R = \frac{\mathbb{E} \left[\sum_{j=1}^m \mathbf{1}\{Y_{n+j} \neq \hat{Y}_{n+j} \text{ and } j \in \mathcal{R}\} \right]}{\mathbb{E} \left[\sum_{j=1}^m \mathbf{1}\{j \in \mathcal{R}\} \right]},$$

which is also known as the marginal false discovery rate (mFDR) in hypothesis testing. In the literature, FDR control is generally preferred over mFDR control. We provide a discussion of mFDR and FDR control in Appendix I.4.

H. Extension to Regression Tasks

While our primary focus is on classification, Conformal Labeling can be naturally extended to regression settings. Consider a loss function $L(Y, \hat{Y})$ that quantifies prediction error—for instance, the squared error $L(Y, \hat{Y}) = (Y - \hat{Y})^2$ —alongside a user-specified tolerance level ϵ . For each test sample, we define the null and alternative hypotheses as:

$$H_0^j : L(Y_{n+j}, \hat{Y}_{n+j}) > \epsilon \quad \text{versus} \quad H_1^j : L(Y_{n+j}, \hat{Y}_{n+j}) \leq \epsilon.$$

This framework generalizes the classification setting, which corresponds to the special case where $L(Y, \hat{Y}) = \mathbf{1}\{Y \neq \hat{Y}\}$ and $\epsilon = 0$. To apply Conformal Labeling in regression, we need an uncertainty score that reflects the model’s predictive uncertainty. While uncertainty score functions are straightforward in classification tasks (e.g., $1 - \max_{y \in \mathcal{Y}} f_y(X)$), regression requires alternative approaches to get an uncertainty score function. For example, when using LLMs, we can leverage their verbalized confidence or prompt them to output prediction intervals, using the interval width as the uncertainty score. The complete procedure for Conformal Labeling in the regression task is outlined in Algorithm 2.

We evaluate Conformal Labeling on two regression problems: sentiment analysis with GPT-4o and protein structure prediction with AlphaFold. We use the data provided by (Candès et al., 2025). For sentiment analysis, we prompt GPT-4o to output a prediction interval $[a_i, b_i]$ for each target Y_i , set the predicted value as $\hat{Y}_i = (a_i + b_i)/2$, and use the interval length $U_i = b_i - a_i$ as the uncertainty score. For protein structure prediction, we take experimentally derived structures as ground truth and AlphaFold predictions as \hat{Y}_i . Uncertainty scores are obtained from AlphaFold’s internal confidence measure, the average predicted local distance difference test (pLDDT). For both experiments, we employ the L2 loss function.

In Table 7, we report the performance of Conformal Labeling on regression tasks with $\alpha = 0.1$. In all cases, Conformal Labeling consistently controls the realized FDR below the target level, while a larger loss threshold ϵ leads to higher power.

Table 7. Performance of Conformal Labeling on regression tasks at $\alpha = 0.1$. Results are shown for sentiment analysis (top) and protein folding (bottom) under different values of the tolerance parameter ϵ . In all cases, Conformal Labeling controls the realized FDR below the target level.

Dataset	Metric	Method		
		CL ($\epsilon = 0.05$)	CL ($\epsilon = 0.06$)	CL ($\epsilon = 0.07$)
Sentiment analysis	FDR (%)	8.48%	8.60%	7.89%
	Power (%)	5.04%	53.14%	94.92%
		CL ($\epsilon = 1$)	CL ($\epsilon = 4$)	CL ($\epsilon = 9$)
Protein folding	FDR (%)	9.67%	9.90%	9.04%
	Power (%)	27.24%	49.73%	97.90%

Table 8. Performance of Conformal Labeling under varying severity levels of ImageNet-C Brightness corruption. "No shift" denotes that the test dataset also comes from ImageNet. Conformal Labeling maintains stable FDR control close to target levels while power decreases with increasing corruption severity.

Test Dataset	Accuracy (%)	$\alpha = 0.05$		$\alpha = 0.1$	
		FDR (%)	Power (%)	FDR (%)	Power (%)
No shift	73.29	5.00	72.27	9.85	79.62
Severity 1	68.98	5.88	65.08	11.74	81.36
Severity 2	67.17	5.87	63.55	11.77	80.12
Severity 3	64.15	5.94	61.52	11.70	78.05
Severity 4	59.30	5.62	57.31	11.67	75.14
Severity 5	52.75	5.56	53.94	11.75	72.09

I. Extensive Study

I.1. Discussion of distribution shift

We emphasize that the calibration set is sampled i.i.d. from a large unlabeled dataset (a **transductive** setting), leaving the remaining data for testing. Given a large unlabeled dataset, we first annotate a small subset as the calibration set, then apply conformal labeling to guarantee the quality of AI labeling. This process ensures that the calibration and test sets are naturally i.i.d., satisfying the standard assumptions of conformal labeling. In other words, Conformal Labeling generally does not encounter distribution shift in practice.

While our method cannot provide theoretical guarantees under distribution shift, we add an experiment with ResNet34 on ImageNet and ImageNet-C Brightness to evaluate its empirical performance. In particular, we use ImageNet as the calibration set and ImageNet-C Brightness with varying severities as the testing set. We present the performance of our method across various testing sets in table 8. The results show that the realized power of our method is getting worse with a higher severity of distribution shift (may be due to the degraded accuracy), while the FDR is relatively insensitive. This demonstrates that our method is empirically robust to moderate distribution shift.

Besides, we note that prior work (Jin & Candès, 2025) has investigated approaches for handling covariate shifts in conformal novelty detection and conformal selection. The same idea can be naturally incorporated into our Conformal Labeling procedure, enabling it to maintain false discovery rate control under covariate shift. We believe it can be an interesting direction for subsequent works if there are some realistic scenarios with distribution shift.

I.2. Comparison of different score functions

The choice of score function only affects the power but not the strict FDR control We present the results of three score functions on the ImageNet dataset in Table 9. While MSP, Energy, and D_α scores lead to vastly different power, all three successfully control the FDR below the target levels (5% and 10%). Specifically, MSP and D_α achieve high power (64% and 80% for $\alpha = 5\%$ and 10%, respectively), whereas Energy yields significantly lower power (11.83% and 50.58%). This demonstrates that a poor score function can incur higher data collection costs by lowering power, but it does not compromise the statistical guarantee of FDR control.

Table 9. Comparison of FDR control and power for MSP, Energy, and D_α score functions. The experiment is conducted with a ResNet-34 model on ImageNet. **Bold** indicates the highest power under the target FDR level. All methods maintain FDR close to target levels, while MSP and D_α achieve significantly higher power than the Energy score.

Method	Target FDR = 5%		Target FDR = 10%	
	FDR (%)	Power (%)	FDR (%)	Power (%)
MSP	4.97	63.87	9.97	80.01
Energy	4.86	11.83	9.94	50.58
D_α	4.95	63.80	9.92	79.74

I.3. Impact of prediction accuracy

Higher prediction accuracy enables better selection results. The performance of Conformal Labeling depends heavily on the underlying prediction accuracy, which is influenced by model capacity and dataset difficulty. We evaluate Conformal Labeling with Qwen3-8B, Qwen3-14B, and Qwen3-32B, whose increasing scales provide greater capacity. MMLU-Pro, more challenging than MMLU, results in lower prediction accuracy. Figure 4 presents the evaluation results. In all cases, the FDR remains below and close to $\alpha = 0.1$. Higher accuracy—achieved with stronger models or easier datasets—boosts power and the AI-labeled ratio. Specifically, for any given model, performance is superior on MMLU compared to MMLU-Pro. Similarly, for each dataset, larger models yield greater power and AI-labeled ratios. Overall, higher prediction accuracy leads to better selection results by achieving higher power and AI-labeled ratio with controlled FDR.

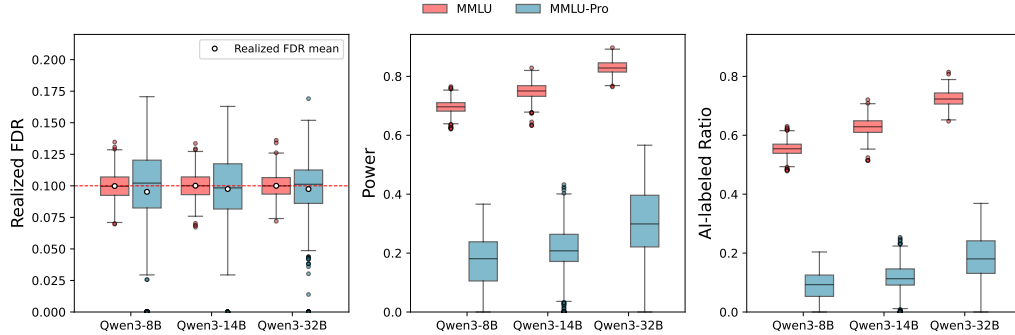


Figure 4. Performance comparison of Conformal Labeling across models of varying accuracy. We employ Qwen3-8B, Qwen3-14B, and Qwen3-32B (model accuracy increases with parameter count) on MMLU and MMLU-Pro with $\alpha = 0.1$. The results show that model with higher accuracy achieves greater power and AI-labeled ratio.

I.4. Discussion of mFDR control and FDR control.

In the labeling task, the mFDR is defined as:

$$\text{mFDR} = \frac{\mathbb{E} \left[\sum_{j=1}^m \mathbf{1}\{Y_{n+j} \neq \hat{Y}_{n+j} \text{ and } j \in \mathcal{R}\} \right]}{\mathbb{E} \left[\sum_{j=1}^m \mathbf{1}\{j \in \mathcal{R}\} \right]},$$

while FDR is defined as

$$\text{FDR} = \mathbb{E} \left[\frac{\sum_{j=1}^m \mathbf{1}\{Y_{n+j} \neq \hat{Y}_{n+j} \text{ and } j \in \mathcal{R}\}}{\max \left\{ \sum_{j=1}^m \mathbf{1}\{j \in \mathcal{R}\}, 1 \right\}} \right].$$

There has been an exhaustive discussion of FDR and mFDR control. For example, Benjamini & Hochberg (1995) proposed the concept of FDR in favor of mFDR, because the latter is impossible to control in the global null case (Gu et al., 2024); Storey (2003) also pointed out that mFDR cannot be used for controlling the joint behavior of the numerator (number of false selections) and the denominator (number of selections).

Table 10. Comparison of different selection methods at target error levels $\alpha = 0.05$ and $\alpha = 0.10$. Conformal Labeling achieves the highest power and the tightest FDR control among the three methods.

Method	$\alpha = 0.05$		$\alpha = 0.10$	
	FDR (%)	Power (%)	FDR (%)	Power (%)
Confidence threshold	2.80	57.23	3.94	66.60
FDR search	4.51	63.11	9.65	75.90
Conformal Labeling	5.00	72.27	9.97	79.91

Table 11. Selection results of conformal labeling with target FDR $\alpha = 0.1$.

Classifier	FDP (%)	Selection Size
KNN ($k = 5$)	9.72	6,142
MLP (100, 25)	8.85	5,715
XGBoost	9.56	4,006

I.5. Comparison to selective prediction with calibrated confidences.

Conformal Labeling achieves higher power than baselines under the same target FDR level. To compare our method with selective prediction with calibrated confidences, we conduct a new experiment on ImageNet using a calibrated ResNet-34 classifier. In particular, we use a holdout dataset to learn an optimal temperature parameter for temperature scaling, achieving an ECE of 2.22%. Given an error level α , we compare Conformal Labeling with two heuristic baselines. **(1) Confidence threshold.** Given a target error level α , an instance is selected if its calibrated maximum softmax probability (MSP) satisfies $\mathcal{S}(x) > 1 - \alpha$. **(2) FDR search.**

We present the results of our method and two baselines in Table 10 below. The results show that Conformal Labeling consistently achieves the highest power and tightest FDR control among the three methods, showing that our method reliably increases the selected set size at the same target false discovery rate. Notably, we emphasize that the two heuristic baselines cannot provide any rigorous guarantee for the FDR control. We believe this demonstrates the benefits of our method compared to the baselines.

I.6. End-to-End Experiment with Conformal Labeling

To assess whether Conformal Labeling can facilitate training a better downstream model, we conduct an end-to-end experiment that integrates label selection with classifier retraining. Specifically, we evaluate whether the samples selected by conformal labeling can effectively augment the training set and improve prediction performance. We adopt a synthetic dataset in this experiment to enable a controlled evaluation setting. In particular, synthetic data allows us to generate a sufficiently large number of i.i.d. samples from a fixed distribution, which allows us to better analyze the end-to-end behavior of conformal labeling.

We generate a synthetic 10-class classification dataset with 27,000 samples using scikit-learn’s `make_classification` function. The dataset is randomly partitioned into three disjoint subsets:

- D_1 : 2,000 samples used to train the initial labeling model;
- D_2 : 20,000 samples used for AI labeling;
- D_3 : 5,000 samples reserved for evaluation.

We first train a base classifier on D_1 . From D_2 , we randomly select 2,000 labeled samples as calibration data and apply conformal labeling with a FDR of $\alpha = 0.1$ to the remaining 18,000 unlabeled samples. This procedure yields an AI-labeled subset D_{label} . We repeat this process using three different base classifiers: KNN, MLP, and XGBoost. Table 11 reports the empirical false discovery proportion (FDP) and the number of selected samples for each classifier. In all cases, the observed FDP is well controlled below the target level, demonstrating the effectiveness of conformal labeling in selecting reliable pseudo-labeled data. After obtaining D_{label} , we retrain each classifier using the combined dataset $D_1 \cup D_{label}$. Table 12

Table 12. Prediction accuracy on D_3 with and without conformal-labeled samples.

Classifier	Training Set	Accuracy (%)	Improvement (%)
KNN	D_1	64.92	–
	$D_1 \cup D_{\text{label}}$	69.60	+4.68
MLP	D_1	65.68	–
	$D_1 \cup D_{\text{label}}$	68.28	+2.60
XGBoost	D_1	59.80	–
	$D_1 \cup D_{\text{label}}$	60.06	+0.26

compares the prediction accuracy on the held-out evaluation set D_3 between models trained only on D_1 and those trained on the augmented dataset.

The results show that incorporating the selected samples consistently improves downstream performance. For example, when KNN is used as the base classifier, training on $D_1 \cup D_{\text{label}}$ increases test accuracy from 64.92% to 69.60% (+4.68%). Similar gains are observed for MLP (+2.60%) and XGBoost (+0.26%). These findings indicate that conformal labeling enables effective utilization of unlabeled data to train more accurate models under some scenarios.

I.7. Prompt Sensitivity Analysis

To evaluate the sensitivity of our method to prompt design, we conduct experiments using QWEN3-32B on the MMLU dataset with three distinct prompts. In all experiments, the confidence measure is computed using a logits-based approach. The three prompts share identical question and answer content but differ in their phrasing and output format constraints. We describe each prompt in detail below.

Prompt 1. The model is instructed to answer a multiple-choice question by outputting only the correct option without any additional text or explanation:

```

The following are multi choice questions. Give ONLY the correct option, no other
words or explanation:
Question: {question}
A: {choice1}
B: {choice2}
C: {choice3}
D: {choice4}
Answer:

```

Prompt 2. The model is explicitly asked to respond with only the letter corresponding to the correct choice, again without providing explanations:

```

You will be given multiple-choice questions. Respond with ONLY the letter of the
correct choice. No explanations.

```

```
Question: {question}
```

```

A: {choice1}
B: {choice2}
C: {choice3}
D: {choice4}

```

```
Answer:
```

Prompt 3. The model is prompted to output only the correct option, with a different structural layout that groups the answer choices under an “Options” header:

```

Answer the following multiple-choice question. Output ONLY the correct option (A,
B, C, etc.). No other text.

```

Table 13. Performance of our method under different prompt designs on the MMLU dataset.

Prompt	Mean FDR (%)	Mean Power (%)	Error (%)
1	9.97	82.99	21.46
2	9.94	82.58	21.48
3	10.00	79.18	22.10

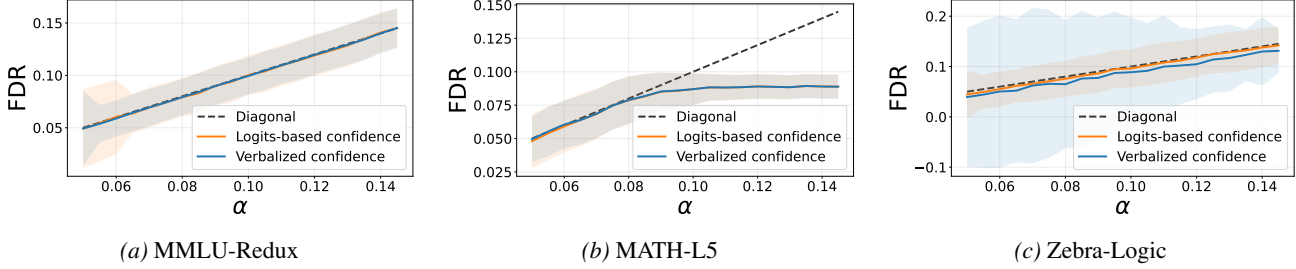


Figure 5. **Empirical FDR of Conformal Labeling across target levels.** Results are obtained using Qwen3-4B-Instruct-2507 on three benchmarks. The dashed line indicates the target FDR level α . Shaded areas denote standard deviations.

Question: {question}

Options:
 A: {choice1}
 B: {choice2}
 C: {choice3}
 D: {choice4}

Correct option:

Table 13 reports the performance of our method under the three prompt designs in terms of mean false discovery rate (FDR), mean power, and the testing error of the underlying language model. The results show that the mean FDR remains consistently close to the nominal level across all prompt designs, indicating that the FDR guarantee of our method is largely insensitive to prompt formulation. Besides, we notice that prompt 3 leads to lower power than the other two prompts. This is because the LLM achieves a higher testing error with this prompt. In summary, our method can be employed by LLM with different prompts.

J. Additional experimental results

In Figure 5, we present the realized FDR of Conformal Labeling under different target level on three benchmarks. The results show that across different target level, Conformal Labeling tightly controls the FDR in the open-ended generation tasks.

We present the reliability diagrams of Qwen3-4B-Instruct-2507 on MMLU-redux, MATH-L5, and Zebra-Logic in Figure 6. The results show that logits-based confidence achieves lower ECE than verbalized confidence in all datasets except for Zebra-Logic, indicating superior reliability of logits-based confidence.

We present the p -value distribution of Qwen3-4B-Instruct-2507 using logits-based and verbalized confidence in Figure 7. The results show that the logits-based score provides a clearer separation between incorrect and correct predictions in most datasets.

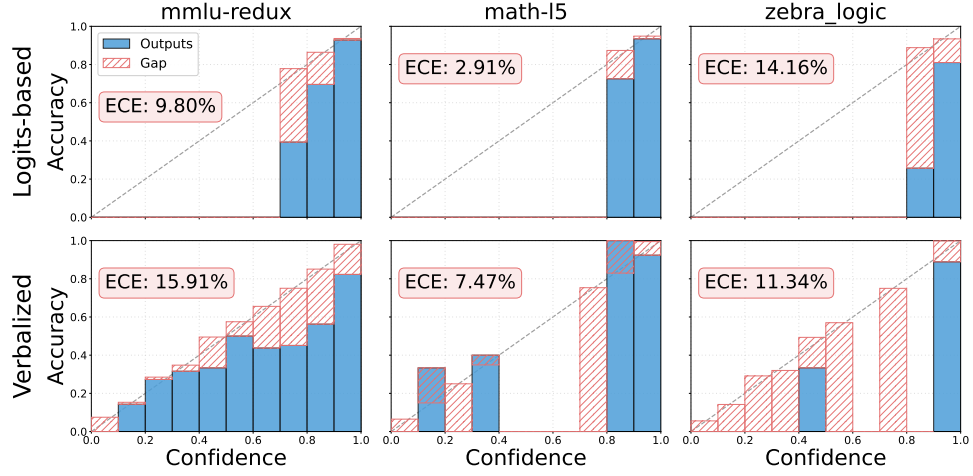


Figure 6. Reliability diagrams of Qwen3-4B-Instruct-2507 across three benchmark datasets (MMLU-Redux, MATH-L5, and Zebra-Logic). Each column corresponds to a dataset. The top row uses logits-based confidence, while the bottom row uses verbalized confidence.

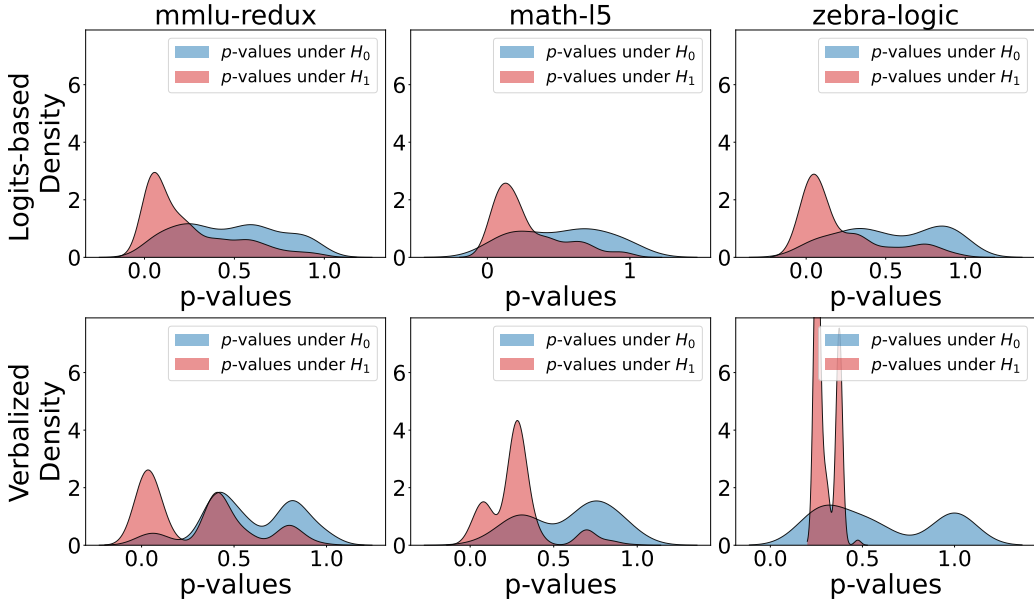


Figure 7. p -value distribution of Qwen3-4B-Instruct-2507 under different uncertainty score functions across three benchmark datasets. Each column corresponds to a dataset. The top row uses logits-based confidence, while the bottom row uses verbalized confidence.